PHYSICAL REVIEW A **81**, 043805 (2010)

Jahn-Teller instability in dissipative quantum systems

Charles P. Meaney, Tim Duty, Ross H. McKenzie, and G. J. Milburn
Department of Physics, School of Mathematical and Physical Sciences, The University of Queensland, St Lucia, Queensland 4072, Australia
(Received 17 June 2009; published 6 April 2010)

We consider the steady states of a harmonic oscillator coupled so strongly to a two-level system (a qubit) that the rotating wave approximation cannot be made. The Hamiltonian version of this model is known as the $E \otimes \beta$ Jahn-Teller model. The semiclassical version of this system exhibits a fixed-point bifurcation, which in the quantum model leads to a ground state with substantial entanglement between the oscillator and the qubit. We show that the dynamical bifurcation survives in a dissipative quantum description of the system, amidst an even richer bifurcation structure. We propose an experimental implementation of this model based on a superconducting cavity: a superconducting junction in the central conductor of a coplanar waveguide.

DOI: 10.1103/PhysRevA.81.043805 PACS number(s): 42.50.Wk, 85.85.+j, 82.40.Bj, 84.40.Dc

I. INTRODUCTION

Circuit quantum electrodynamics [1] has emerged in the past few years as a new experimental context for the study of strongly coupled quantum systems. A superconducting coplanar microwave cavity can support very strong electric fields with very low dissipation. The electric field due to a single photon can be as large as 0.2 V/m, and cavity quality factors as high as 10^6 have been obtained [2]. Large electric dipoles, in the form of superconducting junction elements, can be placed into the gap between the central conductor and the ground plane and coupled into the cavity field, which is treated as a simple harmonic oscillator. The coupling strength can now be made far larger than equivalent experiments in atomic physics, and may yet be made still larger [1]. In this situation we cannot make the rotating wave approximation that is standard in quantum optics. The interaction Hamiltonian that describes this system is known as the $E \otimes \beta$ Jahn-Teller model. In the case of superconducting qubits, dissipation cannot be neglected. In this paper we make a detailed study of the effect of dissipation on the Jahn-Teller instability both in the classical and the quantum description.

The $E \otimes \beta$ Jahn-Teller model describes the interaction between a single harmonic oscillator and a two-level system, or qubit [3]. There is a critical coupling strength at which the nature of the ground state undergoes a qualitative change reflecting a bifurcation in a fixed point of the corresponding classical model [4]. As the coupling strength increases, the entanglement (in the ground state) between the qubit and the oscillator increases monotonically. Starting from zero coupling strength and increasing to very large coupling, the ground states change from

$$|0\rangle_c|0\rangle_q \rightarrow |\alpha\rangle_c|+\rangle_q + |-\alpha\rangle_c|-\rangle_q, \tag{1}$$

where $|0\rangle_c$ and $|0\rangle_q$ are the bare cavity oscillator and qubit ground states and $|\pm\alpha\rangle_c$ is an oscillator coherent state centered at α, which increases with the coupling strength, while $|\pm\rangle_q$ are orthogonal qubit states. The rate of change of entanglement as a function of the coupling strength is greatest for coupling strengths near the critical coupling strength for a fixed-point bifurcation in the corresponding semiclassical description [4]. This has significant implications for the ability to reach the zero photon state in the cavity by cooling. If the bifurcation were to survive the inclusion of damping (and we show it does) one could engineer a system with a coupling strength above the critical value so that cooling the device would reach a steady state in which the number of photons in the field was $|\alpha|^2$ and not zero, as it would be if the coupling was weak, while the qubit would be measured to be in a totally mixed state for α only a little larger than unity. As real systems have finite damping, no matter how small, it is our objective here to determine to what extent the ground-state bifurcation exhibited in the conservative system is manifest in the damped system as a bifurcation of the steady state and, further, to specify experimental scenarios in circuit QED in which it may be observed.

The paper is structured as follows. In Sec. II we present a detailed analysis of the fixed-point structure of the dissipative Jahn-Teller $E \otimes \beta$ model in a semiclassical description. We include both dissipation of the oscillator and the two-level system. Surprisingly, despite the large number of parameters in the mode, the bifurcation structure is shown to depend on only three dimensionless independent parameters. In Sec. III we consider the quantum version of the model in which dissipation is described using a Markov master equation of the oscillator and the two-level system. We numerically determine the steady state of the system. After tracing out the two-level system, we construct the Q function for the oscillator. We then show that as the control parameters are varied through the values at which the semiclassical model shows bifurcations the Q function changes from being single-peaked to double-peaked with support on the semiclassical fixed points. In Sec. IV we present a physical system in circuit quantum electrodynamics that could be used to implement the dissipative Jahn-Teller model. We suggest a number of key experimental signatures of the bifurcation. Finally, in Sec. V we summarize our results and suggest new directions for further work.

II. THE DISSIPATIVE $E \otimes \beta$ JAHN-TELLER MODEL

We consider the case of a two-level system coupled to a simple harmonic oscillator. The coupling is linear in the oscillator displacement and represents a state-dependent constant force acting on the oscillator. The two-level system Hamiltonian includes a term which mixes the eigenstates of the conditional displacement. In order to model a realistic

device we also need to include dissipation of both the oscillator and the two-level system. The oscillator is damped into a zero-temperature heat bath with an amplitude decay rate of κ. The two-level system is assumed to undergo spontaneous emission at rate γ and phase decay at rate Γ. The irreversible dynamics due to these processes will be described by a master equation for weak damping (and with the rotating wave approximation for the system-bath coupling), for density matrix ρ of the total resonator and qubit system. This master equation is

$$\begin{aligned}\frac{d\rho}{dt} &= -\frac{\mathrm{i}}{\hbar}[\mathcal{H},\rho] + \kappa(2a\rho a^\dagger - a^\dagger a\rho - \rho a^\dagger a)\\ &\quad + \frac{\gamma}{2}(2\sigma_{-_x}\rho\sigma_{+_x} - \sigma_{+_x}\sigma_{-_x}\rho - \rho\sigma_{+_x}\sigma_{-_x})\\ &\quad - \frac{\Gamma}{8}[\sigma_x,[\sigma_x,\rho]],\end{aligned} \tag{2}$$

where

$$\mathcal{H} = \hbar\omega a^\dagger a + \frac{\hbar\Delta}{2}\sigma_x + \frac{\hbar\epsilon}{2}\sigma_z + \hbar\lambda(a+a^\dagger)\sigma_z + \hbar\eta(a+a^\dagger) \tag{3}$$

and

$$\sigma_{\pm_x} = \tfrac{1}{2}(\sigma_z \mp \mathrm{i}\sigma_y), \tag{4}$$

where σ_x etc. are Pauli matrices; Δ and ϵ give the strength of the transverse and bias fields on the qubit; λ is the strength of the coupling between the oscillator and the qubit; and η is a coherent driving of the oscillator. The frequency of the harmonic oscillator is ω. In Sec. IV we will mention a physical implementation of this Hamiltonian based on a circuit quantum electrodynamic implementation in which a qubit based on a Josephson tunneling device is coupled to a superconducting microwave resonator, realizing the two-level system and oscillator, respectively. In this section will we keep the oscillator and qubit and their Hamiltonian coupling constants arbitrary.

Note that we have modeled dissipation of the qubit as spontaneous emission in the eigenbasis of σ_x. This is based on the assumption that the free Hamiltonian of the qubit is simply proportional to σ_x. This makes our model consistent with the Hamiltonian model discussed in [4], which has no dissipation and $\epsilon = 0$, and ensures that, for this limit, the fixed points of the two models coincide. The coupling between the qubit and the oscillator is modeled by the term proportional to λ and represents a state-dependent force acting on the oscillator. Alternatively, we can think of this term as describing a dependance of the energy eigenstates of the qubit on an oscillator degree of freedom, as occurs in the original Jahn-Teller model in which the electronic energy levels are dependent on one or more relative nuclear coordinate. Finally, we have added an independent resonant force acting on the oscillator degree of freedom through the term proportional to η. In the circuit QED realization this would represent a driving voltage applied to the coplanar cavity.

In the absence of dissipation, the semiclassical equations of motion that follow for the Hamiltonian have a fixed-point pitch-fork bifurcation [4] (for bifurcation types see [5]) at a critical coupling strength of $\lambda_{\mathrm{cr}} = \frac{\sqrt{\Delta\omega}}{2}$. A single stable elliptic fixed point (for fixed point types see [5]), with zero cavity field amplitude below the bifurcation, changes stability to give two new elliptic fixed points with equal and opposite cavity field amplitude. When dissipation is included we expect that a similar bifurcation will occur but in this case the fixed points will be zero-dimensional attractors (i.e., fixed points attracting trajectories passing through nearby regions in phase space). We can study this bifurcation by deriving the semiclassical equations of motion as follows. Using the master equation we construct moment equations for the expectation of each of the two-level system operators (σ_x, σ_y, and σ_z) and for the quadrature phase field operators defined by

$$\begin{aligned}X &= \tfrac{1}{2}(a+a^\dagger),\\ Y &= -\mathrm{i}\tfrac{1}{2}(a-a^\dagger),\end{aligned} \tag{5}$$

which satisfy the commutation relations $[X,Y] = \mathrm{i}/2$. The equations of motion for the expectations of the five quantities of interest are found to be

$$\begin{aligned}\frac{d\langle X\rangle}{dt} &= \omega\langle Y\rangle - \kappa\langle X\rangle,\\ \frac{d\langle Y\rangle}{dt} &= -\eta - \lambda\langle\sigma_z\rangle - \omega\langle X\rangle - \kappa\langle Y\rangle,\\ \frac{d\langle\sigma_x\rangle}{dt} &= -\epsilon\langle\sigma_y\rangle - 4\lambda\langle X\sigma_y\rangle - \gamma(1+\langle\sigma_x\rangle),\\ \frac{d\langle\sigma_y\rangle}{dt} &= -\Delta\langle\sigma_z\rangle + \epsilon\langle\sigma_x\rangle + 4\lambda\langle X\sigma_x\rangle - \frac{\gamma+\Gamma}{2}\langle\sigma_y\rangle,\\ \frac{d\langle\sigma_z\rangle}{dt} &= \Delta\langle\sigma_y\rangle - \frac{\gamma+\Gamma}{2}\langle\sigma_z\rangle.\end{aligned} \tag{6}$$

The equations of motion for the first-order moments couple to the second-order moments, which in turn couple to infinite orders. We define the semiclassical equations by factorizing these second-order moments to get a closed system of equations. Specifically, this means that we make the two assumptions that $\langle X\sigma_x\rangle = \langle X\rangle\langle\sigma_x\rangle$ and $\langle X\sigma_y\rangle = \langle X\rangle\langle\sigma_y\rangle$, or equivalently that the covariances $\langle X,\sigma_x\rangle \ll \langle X\rangle\langle\sigma_x\rangle$ and $\langle X,\sigma_y\rangle \ll \langle X\rangle\langle\sigma_y\rangle$. [An interesting special case arises when $\Delta = 0$. Then equations of motion for $\langle X\rangle$, $\langle Y\rangle$, and $\langle\sigma_z\rangle$ are seen to decouple from those for $\langle\sigma_x\rangle$ and $\langle\sigma_y\rangle$ and consequently higher order moments. This decoupled system of $\langle X\rangle$, $\langle Y\rangle$, and $\langle\sigma_z\rangle$, can be exactly solved. In fact, this can also be seen from the Hamiltonian (3), where Δ is the term producing the coupling between the displaced oscillators.] After factorizing the second-order moments, the semiclassical variables are defined by

$$\begin{aligned}\langle X\rangle &\mapsto x,\\ \langle Y\rangle &\mapsto y,\\ \langle\sigma_x\rangle &\mapsto L_x,\\ \langle\sigma_y\rangle &\mapsto L_y,\\ \langle\sigma_z\rangle &\mapsto L_z.\end{aligned} \tag{7}$$

These yield the semiclassical equations of motion (where a dot indicates a time derivative)

$$\begin{aligned}\dot{x} &= \omega y - \kappa x,\\ \dot{y} &= -\eta - \lambda L_z - \omega x - \kappa y,\\ \dot{L_x} &= -\epsilon L_y - 4\lambda x L_y - \gamma(1+L_x),\end{aligned}$$

$$\dot{L_y} = -\Delta L_z + \epsilon L_x + 4\lambda x L_x - \frac{\gamma+\Gamma}{2}L_y,$$
$$\dot{L_z} = \Delta L_y - \frac{\gamma+\Gamma}{2}L_z, \tag{8}$$

whose steady states must satisfy the Bloch sphere constraints, which depend on the presence or absence of qubit dissipation. If there is no qubit dissipation, the steady states lie on the Bloch sphere, whereas with the presence of qubit dissipation they may lie inside. Thus we have that

$$\begin{aligned} L_x^2 + L_y^2 + L_z^2 &= 1, \quad \text{if} \quad \gamma = \Gamma = 0, \\ L_x^2 + L_y^2 + L_z^2 &\leqslant 1, \quad \text{if} \quad \gamma > 0 \text{ or } \Gamma > 0. \end{aligned} \tag{9}$$

To clarify the meaning of these Bloch sphere constraints, we raise the question of how one should compare quantum stationary states and classical fixed points in Hamiltonian systems. Above the bifurcation in the dissipation-free $E \otimes \beta$ model, the ground state of the quantum Hamiltonian is the entangled state in Eq. (1), while the classical stable fixed points bifurcate into a *pair* of fixed points [explicitly shown later in (18)]. The entangled quantum ground state has support on *both* the fixed points.

The right way to compare the quantum steady-state phase space to the classical description is to consider a classical distribution of points in the classical phase space. Such a distribution is double-peaked on the pair of fixed points but nonetheless has support entirely on the Bloch sphere. However, if we now compute the average of L_x, L_y, L_z for this distribution, we find that the average values lie inside the Bloch sphere in the same way that the corresponding averages do for the entangled quantum state. Of course the classical distributions, while they do reflect the correlations implicit in the fixed-point structure above the bifurcation, are not entangled.

A. Semiclassical fixed-points locations

The semiclassical equations of motion (8) have fixed points ($\dot{x} = \dot{y} = \dot{L}_x = \dot{L}_y = \dot{L}_z = 0$) that satisfy the Bloch sphere constraints (9). These solutions are markedly qualitatively different depending on the presence or absence of qubit dissipation. In fact, there are three qualitatively different semiclassical steady states: no qubit dissipation; qubit dissipation consisting of only dephasing (no spontaneous emission); and qubit dissipation with spontaneous emission. The possible presence of oscillator or cavity decay is included in each of the three categories. The coupling positivities and phases $\omega, \Delta, \lambda > 0, \kappa, \gamma, \Gamma \geqslant 0$, and $\epsilon, \eta \in \mathbb{R}$ will be assumed for all of the following semiclassical analysis.

We also define several convenient dimensionless parameters: the bias or driving parameter ξ; a parameter α dependent on the coupling λ; a parameter β dependent on the magnitude of the qubit dissipation parameters; a parameter δ dependent on the ratio between the two different types of qubit dissipation (spontaneous emission γ and dephasing Γ). We also define two combinations of these parameters: μ and ν. The previous assumptions about coupling positivities imply similar assumptions about these parameters ($\alpha, \mu > 0$ and $\beta, \delta, \nu \geqslant 1$ and $\xi \in \mathbb{R}$). We define the dimensionless parameters (noting that this α is not a coherent state amplitude)

$$\xi = -\frac{\eta}{\lambda} + \frac{\epsilon(\omega^2+\kappa^2)}{4\lambda^2\omega}, \tag{10}$$

$$\alpha = \frac{4\lambda^2\omega}{\Delta(\omega^2+\kappa^2)}, \quad \beta = 1 + \left(\frac{\gamma+\Gamma}{2\Delta}\right)^2, \quad \delta = 1 + \frac{\Gamma}{\gamma}, \tag{11}$$

$$\mu = \delta\alpha = \frac{4\left(1+\frac{\Gamma}{\gamma}\right)\lambda^2\omega}{\Delta(\omega^2+\kappa^2)},$$
$$\nu = \delta\beta = \left(1+\frac{\Gamma}{\gamma}\right)\left(1+\left(\frac{\gamma+\Gamma}{2\Delta}\right)^2\right). \tag{12}$$

We must also consider the stability of the fixed points. The five semiclassical variables can be considered as a vector $\mathbf{x}$, such that about a fixed point $\mathbf{x^0}$ we have

$$\begin{aligned} \boldsymbol{\delta x} &= \mathbf{x} - \mathbf{x^0} \\ &= \left[x - x^0, y - y^0, L_x - L_x^0, L_y - L_y^0, L_z - L_z^0\right]^T, \end{aligned} \tag{13}$$

$$\frac{d}{dt}\boldsymbol{\delta x} = \mathbf{M}\boldsymbol{\delta x}, \tag{14}$$

where the Jacobian matrix $\mathbf{M}$ is

$$\mathbf{M} = \begin{bmatrix} -\kappa & \omega & 0 & 0 & 0 \\ -\omega & -\kappa & 0 & 0 & -\lambda \\ -4\lambda L_y^0 & 0 & -\gamma & -\epsilon - 4\lambda x^0 & 0 \\ 4\lambda L_x^0 & 0 & \epsilon + 4\lambda x^0 & -\frac{\gamma+\Gamma}{2} & -\Delta \\ 0 & 0 & 0 & \Delta & -\frac{\gamma+\Gamma}{2} \end{bmatrix}. \tag{15}$$

Stability of the fixed point requires all the eigenvalues of the Jacobian to have a real part less than or equal to zero [5]. A real part of exactly zero indicates marginal stability in that parameter direction, where the fixed point is neither attractive nor repulsive. Real parts strictly less than zero are attracting fixed points which draw in nearby regions in phase space. In general stability depends on many more coupling parameter combinations than those which define the fixed points. Thus, the stability is generally calculated numerically for fixed points with specific values of all couplings.

In particular, to investigate the change in stability over a large region of parameter space requires random sampling. Where an analytic method is not possible to check the stability of the fixed points we discuss in the following a numerical method. Specifically, random samples are taken from a logarithmic distribution in the bounded eight-dimensional space spanned by $\omega, \Delta, \epsilon, \lambda, \eta, \kappa, \gamma$, and Γ, where each parameter can take a value between 10^{-4} and 10^4. A description of a fixed point as "mostly" stable or unstable with this method will be used to indicate that the vast majority but not all (>99% but <100%) of the random samples taken yielded stable or unstable fixed points, respectively.

1. No qubit dissipation

When qubit dissipation is neglected ($\gamma = \Gamma = 0$, $\kappa \geqslant 0$), there are three classes of semiclassical steady states. Two of these classes require $\xi = 0$; and the other requires $\xi \neq 0$.

Class 1: For $\xi = 0$ there are two fixed points that occur for all parameter values,

$$\begin{aligned} x^0 &= -\frac{\eta\omega}{\omega^2+\kappa^2} = -\frac{\epsilon}{4\lambda}, \\ y^0 &= -\frac{\kappa\eta}{\omega^2+\kappa^2} = -\frac{\kappa\epsilon}{4\lambda\omega}, \\ L_x^0 &= \pm 1, \\ L_y^0 &= 0, \\ L_z^0 &= 0. \end{aligned} \tag{16}$$

The fixed point with $L_x^0 = +1$ is unstable for most coupling values (as determined by the numerical method described), while the fixed point with $L_x^0 = -1$ is stable for most coupling values for $\alpha < 1$ and mostly unstable for $\alpha > 1$.

Class 2: Also for $\xi = 0$ there are two fixed points that only occur for $\alpha > 1$ (note that for $\alpha = 1$ this second class of fixed points is also the first class just described),

$$\begin{aligned} x^0 &= -\frac{\eta\omega}{\omega^2+\kappa^2} \mp \frac{\lambda\omega}{\omega^2+\kappa^2}\sqrt{1-\frac{1}{\alpha^2}} \\ &= -\frac{\epsilon}{4\lambda} \mp \frac{\lambda\omega}{\omega^2+\kappa^2}\sqrt{1-\frac{1}{\alpha^2}}, \\ y^0 &= -\frac{\kappa\eta}{\omega^2+\kappa^2} \mp \frac{\kappa\lambda}{\omega^2+\kappa^2}\sqrt{1-\frac{1}{\alpha^2}} \\ &= -\frac{\kappa\epsilon}{4\lambda\omega} \mp \frac{\kappa\lambda}{\omega^2+\kappa^2}\sqrt{1-\frac{1}{\alpha^2}}, \\ L_x^0 &= -\frac{1}{\alpha}, \\ L_y^0 &= 0, \\ L_z^0 &= \pm\sqrt{1-\frac{1}{\alpha^2}}. \end{aligned} \tag{17}$$

These fixed points can be stable or unstable depending on the coupling values (for example, they are mostly stable for $\kappa = 0$ in our numerical determination). The L_z components of the first two classes of fixed points are plotted in Fig. 1.

Class 3: For $\xi \neq 0$ there are up to four real fixed points dependent on a quartic equation,

$$\begin{aligned} x^0 &= -\frac{\eta\omega}{\omega^2+\kappa^2} - \frac{\lambda\omega}{\omega^2+\kappa^2}L_z^0, \\ y^0 &= -\frac{\kappa\eta}{\omega^2+\kappa^2} - \frac{\kappa\lambda}{\omega^2+\kappa^2}L_z^0, \\ L_x^0 &= -\frac{1}{\alpha}\frac{L_z^0}{L_z^0-\xi}, \\ L_y^0 &= 0, \\ L_z^0 &= L_z^0, \end{aligned} \tag{18}$$

where L_z^0 satisfies the quartic equation [from (9)]

$$\left(L_z^0\right)^2 + \alpha^2\left[\left(L_z^0\right)^2 - 1\right]\left(L_z^0 - \xi\right)^2 = 0. \tag{19}$$

Note that for $\xi \neq 0$, $L_z^0 = \xi$ is never a solution to this equation and so the pole in this expression for L_x^0 is never encountered.

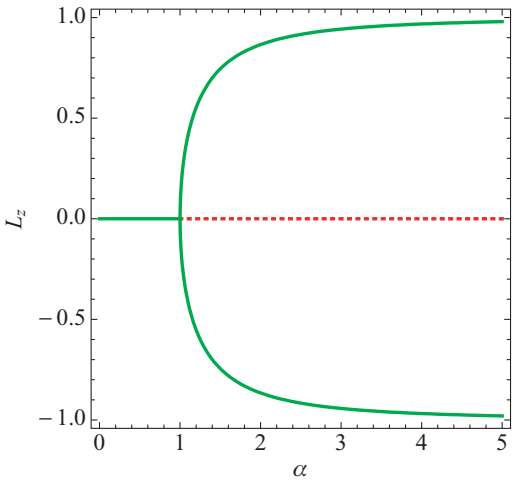

FIG. 1. (Color online) L_z component of the semiclassical steady states as a function of the parameter α for no spontaneous emission or dephasing of the two-level system ($\gamma = \Gamma = 0$) and no driving ($\xi = 0$). There are two solutions along the line $L_z^0 = 0$, one of which is stable for most coupling values (as determined by the numerical method described in the text) for $\alpha < 1$; otherwise, these $L_z^0 = 0$ solutions are mostly unstable. The two new solutions which appear for $\alpha > 1$ have L_z components $L_z^0 = \pm\sqrt{1-\frac{1}{\alpha^2}}$ and can be stable or unstable depending on the coupling values (for example, they are stable for most coupling values when there is no oscillator decay). Hence, depending on the values of the coupling parameters there is often a supercritical pitchfork bifurcation at $\alpha = 1$. The colors in the diagram illustrate a typical case: The solid green lines are stable fixed points, while the dotted red line is unstable.

The L_z component of this third class of fixed points is plotted in Fig. 2. The bifurcations of these fixed points are shown in the bifurcation diagram of Fig. 3. The figure illustrates the contour $\alpha^4\xi^2[(\xi^2-1)^3\alpha^6 + 3(\xi^4+7\xi^2+1)\alpha^4 + 3(\xi^2-1)\alpha^2 + 1] = 0$, along which the bifurcations occur. This analytical expression follows from the discriminant of the quartic equation (19).

2. *Dephasing-only qubit dissipation*

When the qubit dissipation is considered to consist of only phase decay ($\gamma = 0$, $\Gamma > 0$, $\kappa \geqslant 0$), there are two classes of semiclassical steady states. One of these classes requires $\xi = 0$; and the other requires $\xi \neq 0$.

Class 1: For $\xi = 0$ there are infinite fixed points that occur for all parameter values,

$$\begin{aligned} x^0 &= -\frac{\eta\omega}{\omega^2+\kappa^2} = -\frac{\epsilon}{4\lambda}, \\ y^0 &= -\frac{\kappa\eta}{\omega^2+\kappa^2} = -\frac{\kappa\epsilon}{4\lambda\omega}, \\ L_x^0 &= L_x^0, \\ L_y^0 &= 0, \\ L_z^0 &= 0, \end{aligned} \tag{20}$$

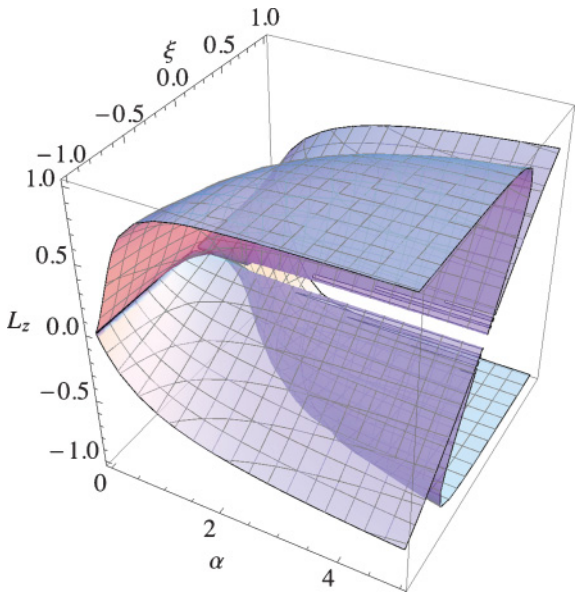

FIG. 2. (Color online) L_z component of the semiclassical steady states as a function of the parameters α and ξ for no spontaneous emission or dephasing of the two-level system ($\gamma = \Gamma = 0$) with driving ($\xi \neq 0$). There are up to four solutions where the L_z components are the real roots L_z^0 of the quartic equation $(L_z^0)^2 + \alpha^2[(L_z^0)^2 - 1](L_z^0 - \xi)^2 = 0$. It is clear that varying either α or ξ can take the solutions through bifurcations. This is shown explicitly in the bifurcation diagram of Fig. 3.

where $(L_x^0)^2 \leqslant 1$. These fixed points can be stable or unstable depending on the coupling values and the choice of L_x^0.

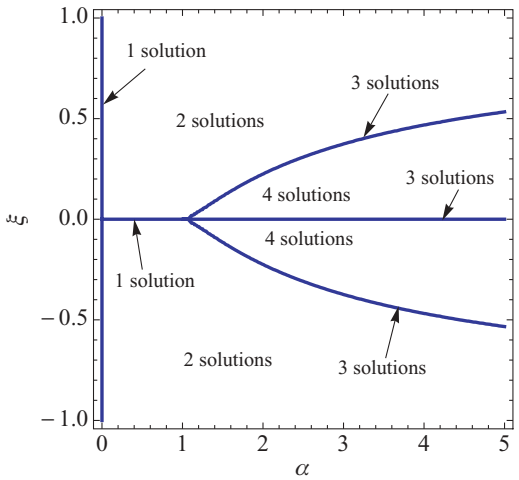

FIG. 3. (Color online) Bifurcation diagram of the semiclassical steady states as a function of the parameters α and ξ for no spontaneous emission or dephasing of the two-level system ($\gamma = \Gamma = 0$) with driving ($\xi \neq 0$). The extra dimension shows that an increase in the magnitude of the driving parameter ξ means that a stronger coupling between the oscillator and two-level system is required to cross the bifurcation. The L_z components of the fixed points are illustrated in Fig. 2 and the bifurcations are clearly visible. Also, the $\xi = 0$ line correctly reflects the bifurcation shown for the no-driving case in figure 1.

Class 2: For $\xi \neq 0$ there is one (trivial) fixed point that occurs for all parameter values,

$$\begin{aligned} x^0 &= -\frac{\eta\omega}{\omega^2+\kappa^2}, \\ y^0 &= -\frac{\kappa\eta}{\omega^2+\kappa^2}, \\ L_x^0 &= 0, \\ L_y^0 &= 0, \\ L_z^0 &= 0. \end{aligned} \tag{21}$$

This fixed point is stable for all coupling values.

3. General qubit dissipation

The general case of qubit dissipation here means with spontaneous emission present ($\gamma > 0, \Gamma \geqslant 0, \kappa \geqslant 0$), in which case there are three classes of semiclassical steady states. Two of these classes require $\xi = 0$; and the other requires $\xi \neq 0$.

Class 1: For $\xi = 0$ there is one fixed point that occurs for all parameter values,

$$\begin{aligned} x^0 &= -\frac{\eta\omega}{\omega^2+\kappa^2} = -\frac{\epsilon}{4\lambda}, \\ y^0 &= -\frac{\kappa\eta}{\omega^2+\kappa^2} = -\frac{\kappa\epsilon}{4\lambda\omega}, \\ L_x^0 &= -1, \\ L_y^0 &= 0, \\ L_z^0 &= 0. \end{aligned} \tag{22}$$

This fixed point is always stable for $\mu < \nu$ and always unstable for $\mu > \nu$.

Class 2: Also for $\xi = 0$ there are two fixed points that only occur for $\alpha > \beta$ (note that for $\alpha = \beta$ this second class of fixed points is also the first class just described),

$$\begin{aligned} x^0 &= -\frac{\eta\omega}{\omega^2+\kappa^2} \mp \sqrt{2}\frac{\lambda\omega}{\omega^2+\kappa^2}\sqrt{\frac{\alpha-\beta}{\delta\alpha^2}} \\ &= -\frac{\epsilon}{4\lambda} \mp \sqrt{2}\frac{\lambda\omega}{\omega^2+\kappa^2}\sqrt{\frac{\alpha-\beta}{\delta\alpha^2}}, \\ y^0 &= -\frac{\kappa\eta}{\omega^2+\kappa^2} \mp \sqrt{2}\frac{\kappa\lambda}{\omega^2+\kappa^2}\sqrt{\frac{\alpha-\beta}{\delta\alpha^2}} \\ &= -\frac{\kappa\epsilon}{4\lambda\omega} \mp \sqrt{2}\frac{\kappa\lambda}{\omega^2+\kappa^2}\sqrt{\frac{\alpha-\beta}{\delta\alpha^2}}, \\ L_x^0 &= -\frac{\beta}{\alpha}, \\ L_y^0 &= \pm\sqrt{2}\sqrt{\beta-1}\sqrt{\frac{\alpha-\beta}{\delta\alpha^2}}, \\ L_z^0 &= \pm\sqrt{2}\sqrt{\frac{\alpha-\beta}{\delta\alpha^2}}. \end{aligned} \tag{23}$$

These fixed points can be stable or unstable depending on the coupling values.

The L_z components of the first two classes of fixed points are plotted in Fig. 4. The bifurcations of these fixed points are shown in the bifurcation diagram of Fig. 5.

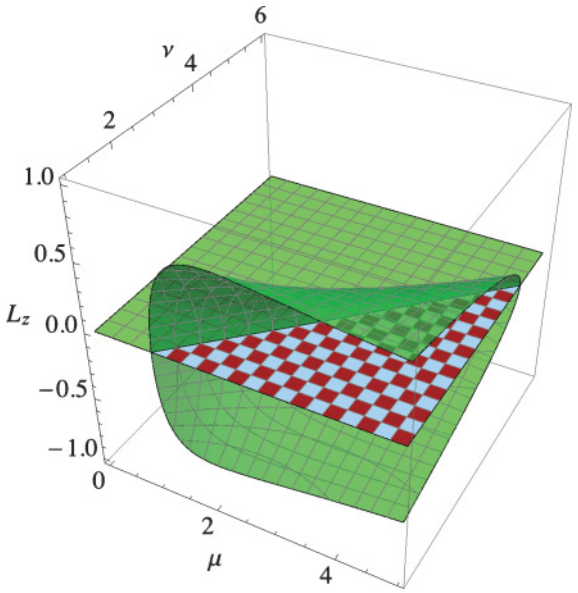

FIG. 4. (Color online) L_z component of the semiclassical steady states as a function of the parameters μ and ν when spontaneous emission is present ($\gamma > 0$) but there is no driving ($\xi = 0$). There is one solution $L_z^0 = 0$ which is always stable for $\mu < \nu$ and always unstable for $\mu > \nu$. The two new solutions which appear for $\mu > \nu$ have L_z components $L_z^0 = \pm\sqrt{2}\sqrt{\frac{\alpha-\beta}{\delta\alpha^2}}$ and can be stable or unstable depending on the coupling values. Hence there is a pitchfork bifurcation along the line $\mu = \nu$ which is often supercritical depending on the coupling parameters. The colors in the diagram illustrate a typical case: The solid green areas are stable fixed points, while the checkered red area is unstable. This bifurcation is shown explicitly in the bifurcation diagram of Fig. 5.

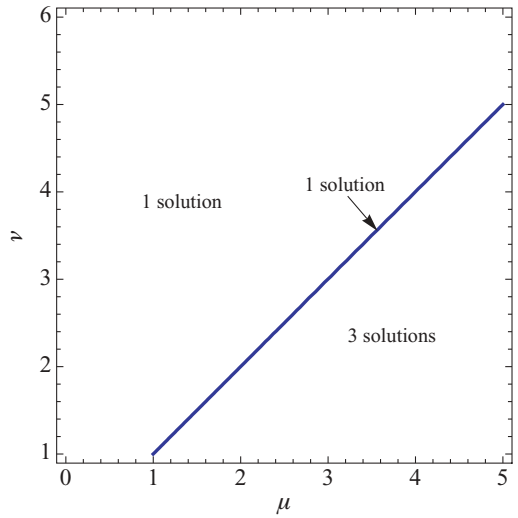

FIG. 5. (Color online) Bifurcation diagram of the semiclassical steady states as a function of the parameters μ and ν when spontaneous emission is present ($\gamma > 0$) but there is no driving ($\xi = 0$). The bifurcations occur along the line $\mu = \nu$. The extra dimension shows that an increase in the qubit dissipation parameter ν means that a stronger coupling between the oscillator and two-level system is required to cross the bifurcation. The L_z components of the fixed points are illustrated in Fig. 4 and the bifurcation is clearly visible.

Class 3: For $\xi \neq 0$ there are up to three real fixed points dependent on a cubic equation,

$$\begin{aligned} x^0 &= -\frac{\eta\omega}{\omega^2+\kappa^2} - \frac{\lambda\omega}{\omega^2+\kappa^2}L_z^0, \\ y^0 &= -\frac{\kappa\eta}{\omega^2+\kappa^2} - \frac{\kappa\lambda}{\omega^2+\kappa^2}L_z^0, \\ L_x^0 &= -\frac{\beta}{\alpha}\frac{L_z^0}{L_z^0-\xi}, \\ L_y^0 &= \sqrt{\beta-1}\,L_z^0, \\ L_z^0 &= L_z^0, \end{aligned} \tag{24}$$

where L_z^0 satisfies the cubic equation

$$\tfrac{1}{2}\mu^2 L_z^0\left(L_z^0-\xi\right)^2 - \mu\left(L_z^0-\xi\right) + \nu L_z^0 = 0. \tag{25}$$

Note that for $\xi \neq 0$, $L_z^0 = \xi$ is never a solution to this equation and so the pole in this expression for L_x^0 is never encountered.

If we consider the third class of fixed points at the forbidden point $\xi = 0$, this third class of fixed points gives the first (except for L_x^0) and second classes of fixed points; hence it generalizes the first two classes in a sense. The L_z component of this third class of fixed points is a function of the three parameters μ, ν, and ξ. The bifurcations of these fixed points are shown in the bifurcation diagram of Fig. 6. The figure illustrates the contour $-2\nu\xi^4\mu^6 + (\mu^2 - 20\nu\mu - 8\nu^2)\xi^2\mu^4 + 8(\mu-\nu)^3\mu^2 = 0$, along which the bifurcations occur. This analytical expression follows from the discriminant of the cubic equation (25).

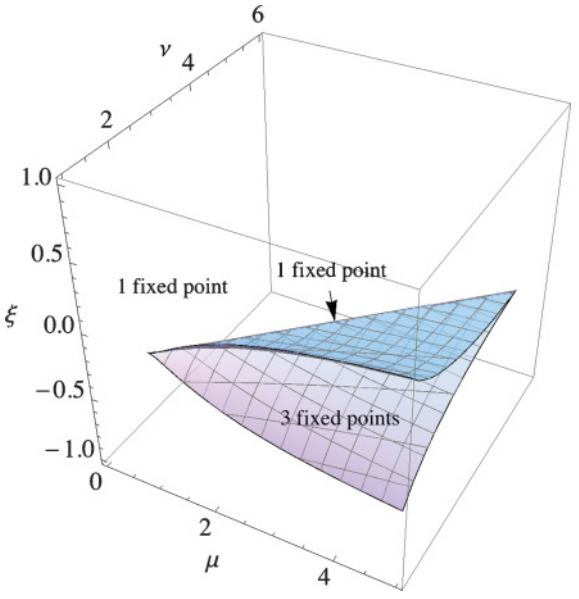

FIG. 6. (Color online) Bifurcation diagram of the semiclassical steady states as a function of the parameters μ and ν when spontaneous emission is present ($\gamma > 0$) with driving ($\xi \neq 0$). The extra dimensions show that an increase in either the qubit dissipation parameter ν or the magnitude of the driving parameter ξ means that a stronger coupling between the oscillator and two-level system is required to cross the bifurcation. Note that the $\xi = 0$ cross section correctly reflects the bifurcation shown for the no-driving case in Fig. 5.

III. QUANTUM STEADY STATES

Knowing the coupling parameter values that result in a semiclassical bifurcation of the steady state solutions, we wish to investigate whether there is a correspondence with the full quantum version. We do this numerically and observe the steady-state phase space of the oscillator as we change the coupling parameters to move through the semiclassical fixed-point bifurcation. It is hoped that our semiclassical analysis of the fixed points can be numerically justified by observing a signature of the semiclassical bifurcation.

Here, we use the quantum optics MATLAB toolbox [6] and pass through two semiclassical bifurcations: one by varying the oscillator-qubit coupling (λ) and another by varying the spontaneous emission (γ). By holding all other couplings equal and ignoring dephasing, varying these two parameters directly corresponds to varying the parameters μ and ν, respectively. Specifically, we set $\omega = 0.01$, $\Delta = 0.1$, $\kappa = 0.001$, $\Gamma = 0$, $\eta = 0$, and $\epsilon = 0$. Thus the three parameters on which the semiclassical bifurcation depends become $\mu = 3960.4\lambda^2$, $\nu = 1 + 25\gamma^2$, and $\xi = 0$. The contour in the bifurcation diagram of Fig. 5 can thus be redrawn as a function of λ and γ. This is done in Fig. 7. The reason for the scale of the coupling values being small is a limitation of our computing power with this numerical method. The oscillator Hilbert space must be truncated to be spanned by a finite number of Fock (number) states. The effect of this is that unless the oscillator state is close to the origin in phase space then the quantum steady state will not be accurately approximated. These coupling values yield steady states which are well approximated in a number basis n of up to $n = 50$. Significantly larger number bases become computationally infeasible on our available hardware. Instead, the solution we have adopted is to appropriately scale the problem such that the bifurcation is close to the origin.

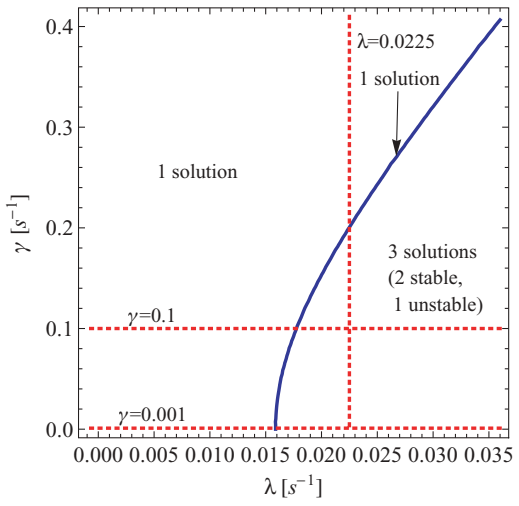

FIG. 7. (Color online) Bifurcation diagram of the semiclassical steady states as a function of the oscillator-qubit coupling parameter (λ) and the qubit spontaneous emission parameter (γ) for the parameters used to numerically calculate the Q functions: The first series of Q functions in Fig. 8 is for λ increasing along the lower horizontal dotted red line $\gamma = 0.001$; the second series of Q functions in Fig. 9 is for λ increasing along the upper horizontal dotted red line $\gamma = 0.1$; and the third series of Q functions in Fig. 10 is for γ increasing along the vertical dotted red line $\lambda = 0.0225$. The other couplings used in the plot above are $\omega = 0.01$; $\Delta = 0.1$; $\kappa = 0.001$; and $\Gamma = \eta = \epsilon = 0$.

The MATLAB quantum optics toolbox gives us a steady-state density matrix for the oscillator-qubit system. From this we can view the steady-state phase space of the oscillator by plotting the Q function for the corresponding reduced density operator of the oscillator. This is defined [7] as the matrix elements of the reduced density operator for the oscillator in the coherent state basis, $Q(\alpha) = \mathrm{tr}(\rho|\alpha\rangle\langle\alpha|)$, where $|\alpha\rangle$ is a oscillator coherent state (and is not to be confused with the dimensionless parameter α determining the position of the semiclassical bifurcation).

Three series of Q functions are plotted by varying λ for two differing fixed values of γ and varying γ for a fixed value of λ. These variations constitute a linear sweep through γ and λ, respectively. The results of these linear sweeps are captured representatively in four data points surrounding the semiclassical bifurcation. These are shown in Figs. 8, 9, and 10, where $\alpha = x + \mathrm{i}y$. The semiclassical bifurcation is clearly evident in each case.

IV. PHYSICAL IMPLEMENTATIONS OF THE JAHN-TELLER MODEL

Devoret *et al.* [1] have proposed a scheme to get ultrastrong coupling between a Cooper-pair box qubit and the microwave field of a coplanar superconducting resonator. The central conductor of the coplanar cavity is divided into two segments separated by a Cooper pair box (see Fig. 11). The quantum theory of such a system begins by first writing down the classical circuit dynamics, constructing a Lagrangian and an associated Hamiltonian. Quantization then proceeds via the usual canonical method. This results in an *effective* quantum theory in which collective variables of direct interest to the experimentalist couple only weakly to the microscopic degrees of freedom, which remain as a source of dissipation and decoherence.

Such devices have recently been demonstrated by the Chalmers group [8]. Another proposal to reach the ultrastrong coupling regime was recently presented by Bourassa *et al.* [9]. They suggest that coupling strengths λ can easily approach several tens of percent of the resonator frequency ω.

If we introduce creation and annihilation operators of the cavity field (the effective flux in the circuit Φ acts as a position, and the effective circuit charge Q as a momentum)

$$\Phi = \mathrm{i}\sqrt{\frac{\hbar\omega L}{2}}(a - a^\dagger),$$
$$Q = \sqrt{\frac{\hbar\omega C_E}{2}}(a + a^\dagger), \tag{26}$$

where

$$\frac{1}{C_E} = \frac{1}{C + C_M} + \frac{1}{C_J},$$
$$\omega = \frac{1}{\sqrt{LC_E}}, \tag{27}$$

and if we consider only the bottom two energy levels for the Josephson junction using Pauli matrices for the resulting qubit,

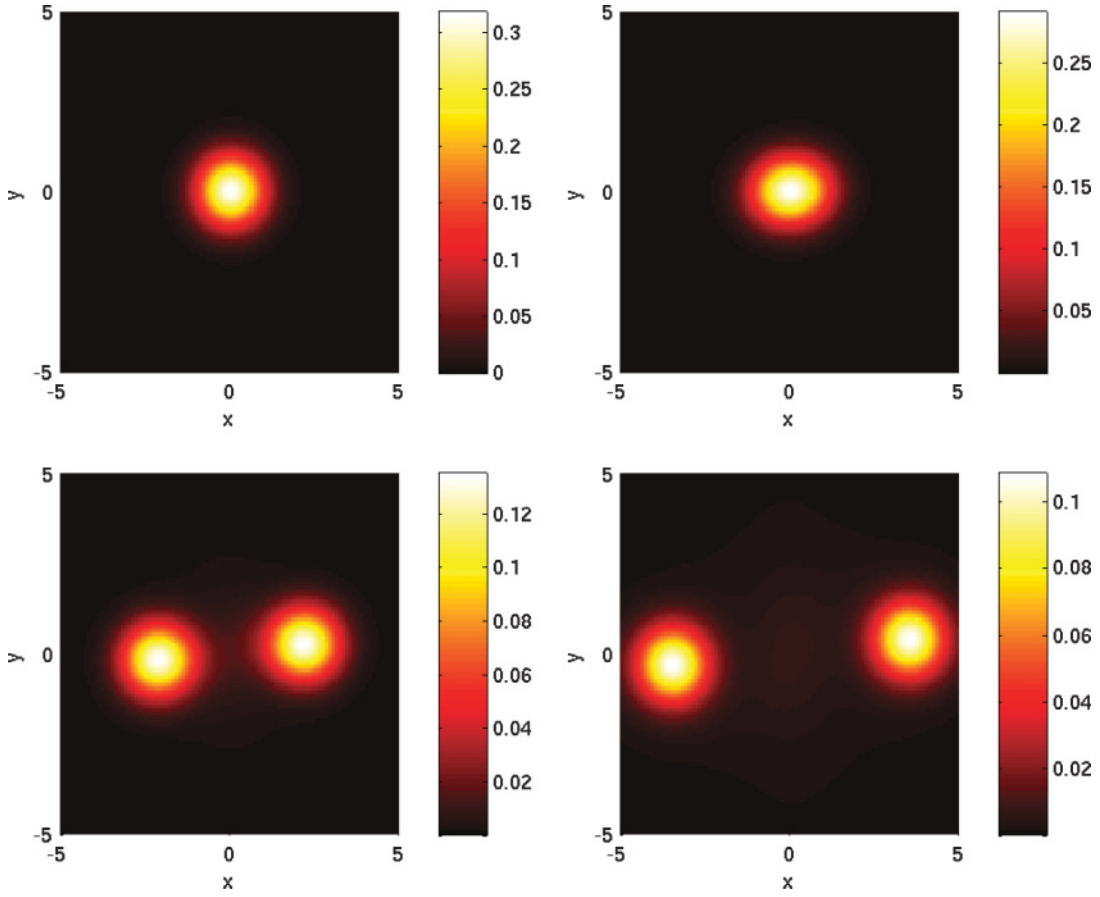

FIG. 8. (Color online) Density plot of Q functions for linearly increasing λ (from 0 to 0.036) along the lower horizontal dotted red line of Fig. 7. The Q function $Q(\alpha)$ is plotted for $\alpha = x + iy$, such that x and y are two quadrature operators of the quantum oscillator modeling the cavity field. The spontaneous emission is $\gamma = 0.0001$, giving a qubit dissipation parameter value of $\nu = 1$. The semiclassical critical value of the oscillator-qubit coupling is $\lambda_c = 0.016$ at the critical parameter value $\mu_c = 1$. The steady-state phase space of the quantum oscillator is seen to undergo a bifurcation which corresponds to the studied semiclassical bifurcation. The specific coupling strengths in the four plots displayed here are $\lambda \approx 0$, 0.01, 0.02, and 0.04, or, equivalently, $\mu \approx 0$, 0.64, 2.34, and 5.13.

then we can rewrite the Hamiltonian (ignoring constant energy offsets) in the Jahn-Teller form of Eq. (3) where, following Devoret *et al.* [1], the coupling is

$$\breve{g} \equiv \frac{2\lambda}{\Delta} = \frac{1}{\sqrt{8\pi}} \left(\frac{E_C}{2E_J}\right)^{1/4} \sqrt{\frac{Z_{\text{vac}}}{Z_C}} \alpha^{-1/2}, \tag{28}$$

with

$$Z_{\text{vac}} = \frac{1}{c\epsilon_0} \approx 377\Omega, \qquad Z_C = \sqrt{\frac{L}{C}}. \tag{29}$$

Here E_J is the Josephson energy for tunneling across the Josephson junction, and E_C is the corresponding charging energy for the Cooper-pair box.

Typically $Z_C = 50\ \Omega$. The proposal of Bourassa *et al.* [9] was based on a three-junction flux qubit. The recent experiment of Paauw *et al.* [10] measured the decay time, T_1, of a three-junction flux qubit as a function of the qubit frequency. They have a considerable range: from $T_1 \sim 10^{-6}$ to 10^{-9} s. Typical T_2 times are half of this. Taking achievable values of $T_1 = 10^{-6}$ s and $T_2 = 0.5 \times 10^{-6}$ s gives dissipation parameters corresponding to $\gamma = 1$ MHz and $\Gamma = 3$ MHz in Secs. III and IV. Taking $E_C/E_J = 200$, Devoret *et al.* [1] arrive at a value of $\lambda \approx 10\Delta$, which is certainly well outside of the domain of validity for the rotating wave approximation. We thus believe this configuration offers a good chance of designing a system with a coupling strength above the Jahn-Teller dissipative bifurcation in circuit QED.

There is one other important issue to mention: The circuit QED system discussed would technically include another Hamiltonian term, the self-energy $\hbar E_C(a + a^\dagger)^2$ (where a and $a^\dagger$ are the annihilation and creation operators of the cavity field) proportional to the charging energy E_C. The Dicke model of quantum optics [11] has a bifurcation with the same double-well potential structure of the $E \otimes \beta$ Jahn-Teller model and this model was shown to bifurcate only when ignoring the self-energy term that arises from the quadratic term in the vector potential in the minimal coupling Hamiltonian of quantum electrodynamics [12]. Furthermore, it has been shown [13] that when the self-energy term is included, the usual atom-cavity system does not develop a double-well potential—the bifurcation does not happen regardless of the strength of the atom-field coupling. Thus, we need to investigate whether the circuit quantum electrodynamic realization

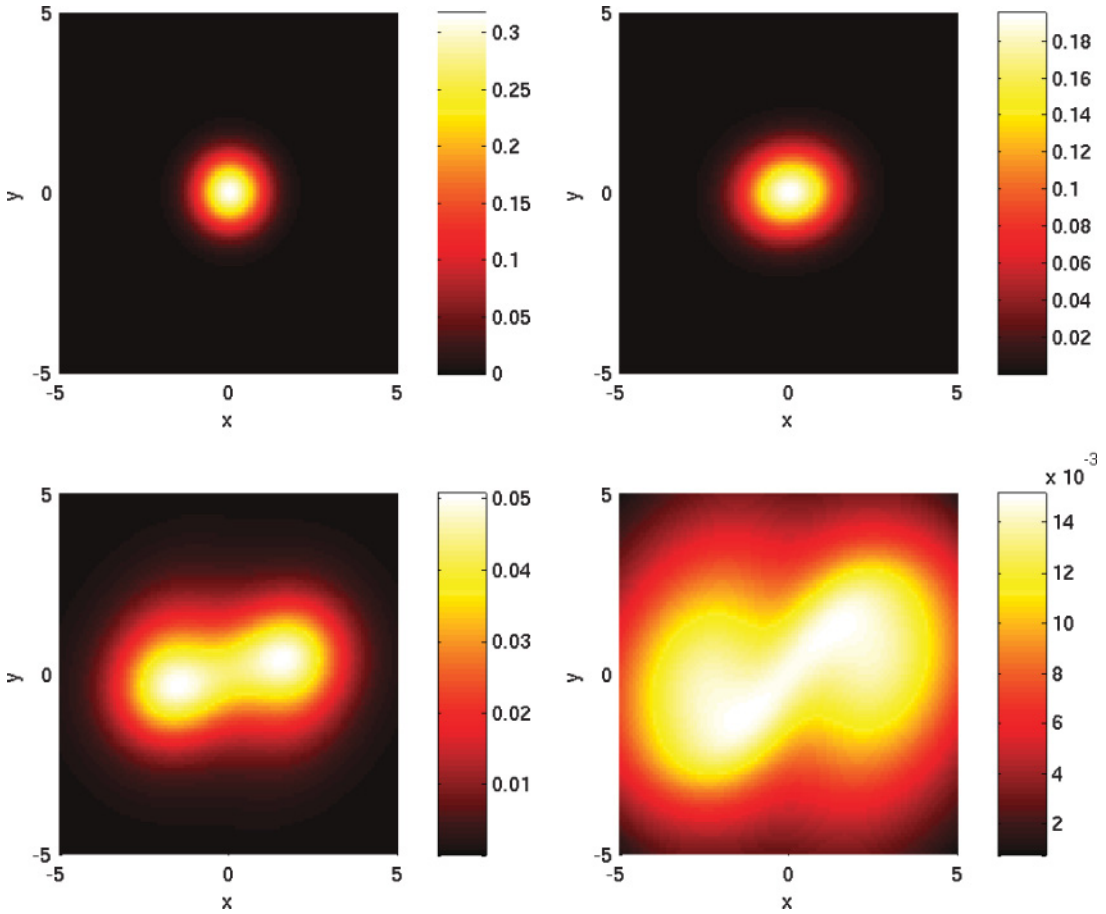

FIG. 9. (Color online) Density plot of Q functions for linearly increasing λ (from 0 to 0.036) along the upper horizontal dotted red line of Fig. 7. The Q function $Q(\alpha)$ is plotted for $\alpha = x + iy$, such that x and y are two quadrature operators of the quantum oscillator modeling the cavity field. The spontaneous emission is $\gamma = 0.1$, giving a qubit dissipation parameter value of $\nu = 1.25$. The semiclassical critical value of the oscillator-qubit coupling is $\lambda_c = 0.018$ at the critical parameter value $\mu_c = 1.25$. The steady-state phase space of the quantum oscillator is seen to undergo a bifurcation which corresponds to the studied semiclassical bifurcation. The specific coupling strengths in the four plots displayed here are $\lambda \approx 0$, 0.01, 0.02, and 0.04, or, equivalently, $\mu \approx 0$, 0.64, 2.34, and 5.13.

of the $E \otimes \beta$ Jahn-Teller model still has a bifurcation when the self-energy term is included.

In the case of the superconducting circuit considered, the self-energy term arises from an often-neglected term in the Hamiltonian $\mathcal{H}_{JJ}$ of the Josephson junction

$$\mathcal{H}_{JJ} = \hbar E_C[n - n_{g0} - \delta n_g(t)]^2 + \hbar E_J \cos\theta, \qquad (30)$$

where n is our Cooper pair number, n_{g0} is the DC component of our gate bias, and $\delta n_g(t)$ is the AC component of the voltage on the central conductor and is treated quantum mechanically, $\delta n_g(t) \propto (a + a^\dagger)$. Expanding the squared bracket gives a term $E_C(\delta n_g)^2$, which is the usually ignored self-energy term $\hbar E_C(a + a^\dagger)^2$. We have investigated the effect of this term on the semiclassical bifurcations derived in Sec. II. The semiclassical bifurcations are exactly as discussed with one modification: The fixed points are still parametrized by three parameters, though one of these parameters requires a slight modification. However, in terms of these parameters, all of the analysis including the defining cubic equation (25) still holds. The necessary modification is the parameter μ, which for an additional Hamiltonian term $\hbar[\Upsilon]4(a + a^\dagger)^2$ changes from

$$\mu = \frac{4\left(1 + \frac{\Gamma}{\gamma}\right)\lambda^2\omega}{\Delta(\omega^2 + \kappa^2)} \rightarrow \mu = \frac{4\left(1 + \frac{\Gamma}{\gamma}\right)\lambda^2\omega}{\Delta(\omega(\omega + \Upsilon) + \kappa^2)}. \qquad (31)$$

Thus, if the self-energy parameter Υ is very large, the parameter μ will remain small even for large λ and never reach the bifurcation point. However, for this circuit QED implementation, the self-energy, which corresponds to the charging energy, is small relative to the frequency of the microwave resonator ω. Typical achievable values for a transmon charge-qubit are $\omega \sim 5$–10 GHz and $E_C \sim 0.35$ GHz [14]. Thus, the effect of the self-energy is only a small shift in the location of the semiclassical bifurcation, and there is no change to its structure. Correspondingly, we have chosen to ignore the term in this paper.

V. CONCLUSION

In this paper we have presented a detailed analysis of the effect of dissipation on the dynamical bifurcation that occurs when there is strong coupling between a single two-level

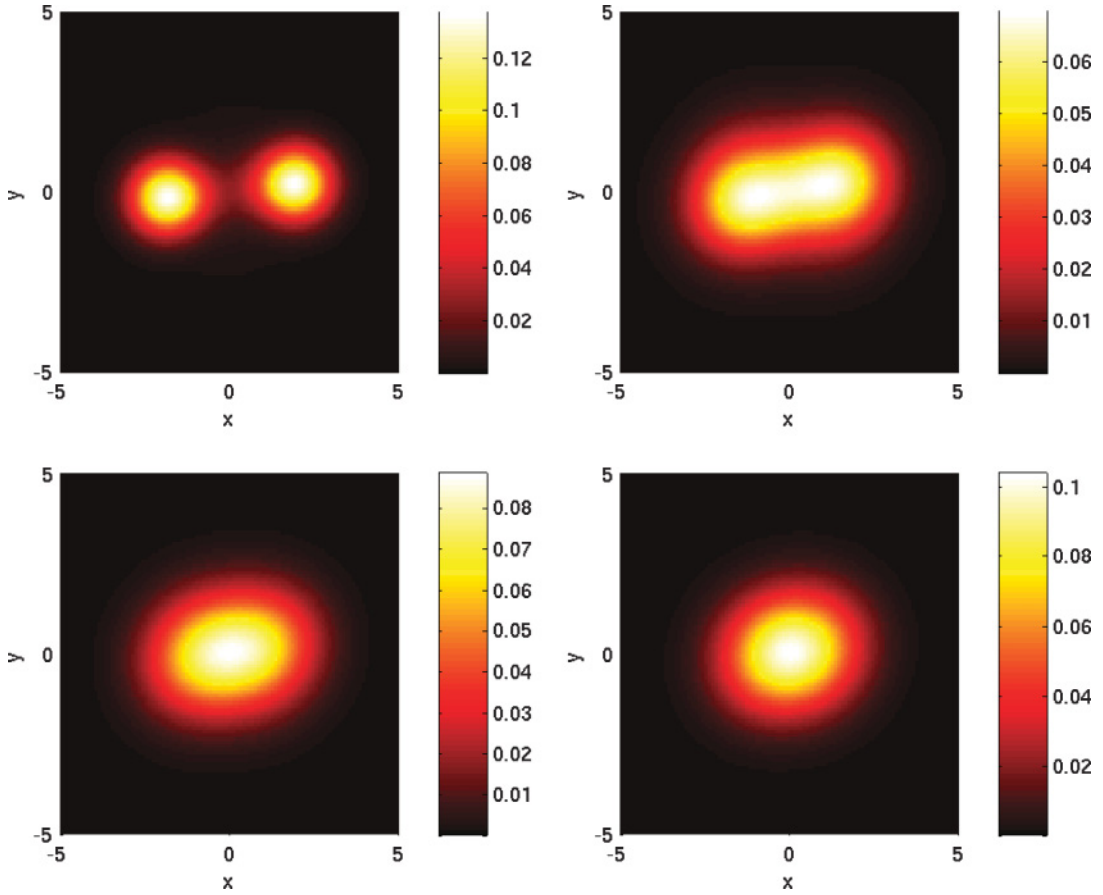

FIG. 10. (Color online) Density plot of Q functions for linearly increasing γ (from 0 to 0.41) along the vertical dotted red line of Fig. 7. The Q function $Q(\alpha)$ is plotted for $\alpha = x + \mathrm{i}y$, such that x and y are two quadrature operators of the quantum oscillator modeling the cavity field. The oscillator-qubit coupling is $\lambda = 0.0225$, giving a parameter value of $\mu = 2.005$. The semiclassical critical value of spontaneous emission is $\gamma_c = 0.2$ at the critical qubit dissipation parameter value $\nu_c = 2.005$. The steady-state phase space of the quantum oscillator is seen to undergo a bifurcation which corresponds to the studied semiclassical bifurcation. The specific dissipation strengths in the four plots displayed here are $\gamma \approx 0$, 0.14, 0.27, and 0.41, or, equivalently, $\nu \approx 1$, 1.47, 2.87, and 5.2.

system and an oscillator: a Jahn-Teller model. We have based our description of dissipation on the physically appropriate mechanisms for the physical realization of the system based on circuit quantum electrodynamics. The key feature of the bifurcation in the dissipative Jahn-Teller model is the change in the oscillator fixed point from one centered on a point of zero radius in phase space to one with support on a nonzero value

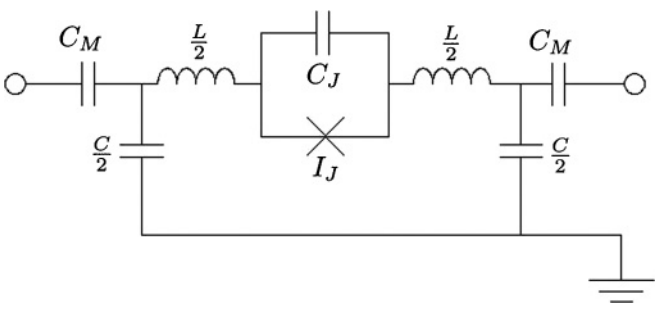

FIG. 11. Lumped element schematic circuit approximation for our proposed circuit QED realization of the $E \otimes \beta$ Jahn-Teller Hamiltonian.

of the radius. This is a distinctly different kind of bifurcation from that discussed recently for the damped nanomechanical Duffing oscillator [15], which only involves a single degree of freedom. In the case considered here, the bifurcation results in steady-state correlations between the state of the oscillator and the two-level system.

As the average excitation energy of an oscillator is proportional to the radius in phase space, this bifurcation would be reflected in a change in the steady-state mean excitation energy from zero to a finite, nonzero value. This would have implications for any attempt to cool the system through tuning to the red sideband transition, that is, tuning the cavity field driving by the mechanical frequency below the cavity frequency. If the parameters were such that the system was already beyond the Jahn-Teller bifurcation, the mechanical system could not be cooled to a zero-phonon state, but it would rather relax to the bistable state with a nonzero mean phonon number. Fluctuations would then drive switching events between the two stable steady states.

The nondissipative model, for coupling stronger than the critical coupling, has a ground state with significant entanglement between the two-level system and the oscillator.

We do not know whether any entanglement remains in the steady state of the dissipative model beyond the bifurcation point. This is a difficult question to answer as the steady state has a non-Gaussian Q function (or Wigner function) and thus it is not clear what would be a good measure of entanglement. In a future work we will use positive P-function methods to attempt to answer this question.

In many implementations of quantum information processing there is often an unwanted strong coupling between an oscillator degree of freedom and a strongly damped two-level system [16,17]. The model of this paper may be relevant to the ongoing study of such systems in those cases where a perturbative treatment of the coupling is not possible.

We have given an example of a circuit quantum electrodynamical system that could exhibit the steady-state bifurcation of the dissipative Jahn-Teller model. Observation of this effect would be a clear demonstration of the ultrastrong coupling regime that can be achieved in these systems, as opposed to what typically happens in atomic systems where the rotating wave approximation eliminates the bifurcation. Such systems open a path to study the quantum signature of nonlinear bifurcations on the steady states of strongly coupled systems.

ACKNOWLEDGMENTS

This work has been supported by the Australian Research Council. We would also like to thank Per Delsing, Andreas Wallraff, and Alexandre Blais for useful discussions (and we now note [9]).

[1] M. H. Devoret, S. Girvin, and R. Schoelkopf, Ann. Phys. (NY) **16**, 767 (2007).
[2] A. Blais, R.-S. Huang, A. Wallraff, S. M. Girvin, and R. J. Schoelkopf, Phys. Rev. A **69**, 062320 (2004).
[3] I. B. Bersuker, *The Jahn-Teller Effect* (Cambridge University Press, Cambridge, 2006).
[4] A. P. Hines, C. M. Dawson, R. H. McKenzie, and G. J. Milburn, Phys. Rev. A **70**, 022303 (2004); J. Larson, *ibid.* **78**, 033833 (2008).
[5] R. C. Hilborn, *Chaos and Nonlinear Dynamics* (Oxford University Press, New York, 1994).
[6] S. M. Tan, Quantum Optics and Computation Toolbox for MATLAB, version 0.15 (2002).
[7] D. F. Walls and G. J. Milburn, *Quantum Optics*, 2nd ed. (Springer, Berlin, 2007), p. 65.
[8] M. Sandberg, C. M. Wilson, F. Persson, T. Bauch, G. Johansson, V. Shumeiko, T. Duty, and P. Delsing, Appl. Phys. Lett. **92**, 203501 (2008).
[9] J. Bourassa, J. M. Gambetta, A. A. Abdumalikov, O. Astafiev, Y. Nakamura, and A. Blais, Phys. Rev. A **80**, 032109 (2009).
[10] F. G. Paauw, A. Fedorov, C. J. P. M. Harmans, and J. E. Mooij, Phys. Rev. Lett. **102**, 090501 (2009).
[11] R. H. Dicke, Phys. Rev. A **93**, 99 (1954).
[12] K. Rzążewski, K. Wódkiewicz, and W. Żakowicz, Phys. Rev. Lett. **35**, 432 (1975).
[13] I. Bialynicki-Birula, and K. Rzążewski, Phys. Rev. A **19**, 301 (1979).
[14] J. Koch, T. M. Yu, J. Gambetta, A. A. Houck, D. I. Schuster, J. Majer, A. Blais, M. H. Devoret, S. M. Girvin, and R. J. Schoelkopf, Phys. Rev. A **76**, 042319 (2007).
[15] I. Kozinsky, H. W. C. Postma, O. Kogan, A. Husain, and M. L. Roukes, Phys. Rev. Lett. **99**, 207201 (2007).
[16] M. Chu, R. E. Rudd, and M. P. Blencowe, e-print arXiv:0705.0015v1.
[17] L. Deslauriers, S. Olmschenk, D. Stick, W. K. Hensinger, J. Sterk, and C. Monroe, Phys. Rev. Lett. **97**, 103007 (2006).